THE JOURNAL OF PHYSICAL CHEMISTRY B

Article

pubs.acs.org/JPCB

Optimization of Triplet Excited State and Singlet Oxygen Quantum Yields of Picolylamine–Porphyrin Conjugates through Zinc Insertion

Betsy Marydasan, Akhil K. Nair, and Danaboyina Ramaiah*

Photosciences and Photonics, Chemical Sciences and Technology Division, CSIR-National Institute for Interdisciplinary Science and Technology (CSIR-NIIST), Trivandrum 695019, India

Supporting Information

ABSTRACT: We synthesized a new class of picolylamine–porphyrin conjugates **1**–**3** and have investigated the effect of heavy atom insertion on their intersystem crossing efficiency through spin–orbit perturbations. By incorporating zinc ions in the core as well as periphery positions of the porphyrin ring, we have successfully optimized their triplet excited state quantum yields and their efficiency to generate singlet oxygen. Uniquely, the picolylamine–porphyrin conjugate **3** having five zinc ions exhibited a triplet excited state quantum yield of ca. 0.97 and a sensitized singlet oxygen generation yield of ca. 0.92. In contrast, the free base porphyrin derivative **1** exhibited ca. 0.64 and 0.5 of the triplet excited state and singlet oxygen quantum yields, respectively. Our results demonstrate that the insertion of zinc metal ions in the picolylamine–porphyrin conjugates not only quantitatively enhances the triplet excited state and singlet oxygen yields but also imparts hydrophilicity, thereby their potential use as sensitizers in photodynamic therapy and green photooxygenation reactions.

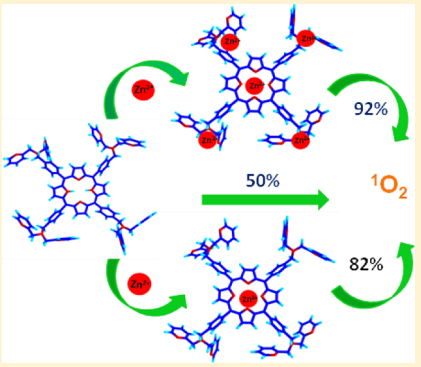

1. INTRODUCTION

Singlet oxygen is one of the most active traits among the reactive oxygen species (ROS) and holds a prominent role in various biological and chemical processes like photodynamic therapy (PDT),[1−3] wet-age related macular degeneration,[4,5] wastewater treatment in environmental chemistry, and photooxygenation reactions in fine chemical industry.[6−8] The chemistry of singlet oxygen differs from that of molecular oxygen, since it is an efficient electrophilic oxidant to several electron rich organic substrates.[9,10] The generation of singlet oxygen through photosensitization by using a photosensitizer in the presence of molecular oxygen has been an active area of research because of their extensive applications. For this purpose, a series of photosensitizers have been reported in the literature, and some of these sensitizers include methylene blue, rosebengal, xanthene, and porphyrin derivatives.[11−13] Among these, the porphyrin derivatives have been extensively employed for singlet oxygen generation and achieved a promising role due to their favorable photophysical properties.[14,15] Of the various porphyrin systems reported, tetraphenylporphyrin (TPP) has been effectively used for photooxygenation reactions using visible light irradiation.[16] However, TPP possesses certain disadvantages such as low singlet oxygen generation efficiency, photodegradation, and poor solubility in aqueous medium, which limit its biological and photooxygenation applications.[17,18]

To improve the singlet oxygen generation efficiency, efforts have been made to modify the sensitizers based on porphyrin systems either by halogenation or metal ion incorporation. For example, Kenneth and co-workers have reported several porphyrin derivatives having a zinc metal ion in the core.[19] These systems unusually showed reduced singlet oxygen yields when compared to the corresponding free base porphyrins. The authors have attributed these observations to the enhanced internal conversion as well as the increased rate of back intersystem crossing (ISC) to the ground state. In another report, Arnaut and co-workers have developed novel sensitizers based on porphyrins and bacteriochlorins having halogen atoms like chlorine, bromine, and zinc metal ion in the core. These systems showed favorable absorption properties as well as enhanced triplet excited states and singlet oxygen quantum yields.[20,21] The increase in generation of singlet oxygen has been attributed to the high intersystem crossing efficiency due to the presence of heavy metal ions. Among them, bacteriochlorin derivative ($TDCPBSO_3H$) showed good solubility in the aqueous medium, thereby demonstrating its potential use in biological applications. Recently, Baptista et al. have reported a novel series of the porphyrin derivatives. These systems on zinc metal ion incorporation showed a negligible effect on their intersystem crossing efficiency as well as singlet oxygen generation.[22,23] In this context, the development of the porphyrins, which generate singlet oxygen efficiently as well as show good solubility in aqueous medium and photostability, is quite challenging for their applications in PDT and photooxygenation reactions.

Received: July 29, 2013
Revised: September 24, 2013
Published: September 24, 2013

Chart 1. Structure of the Picolylamine−Porphyrin Conjugates 1−3 under Investigation

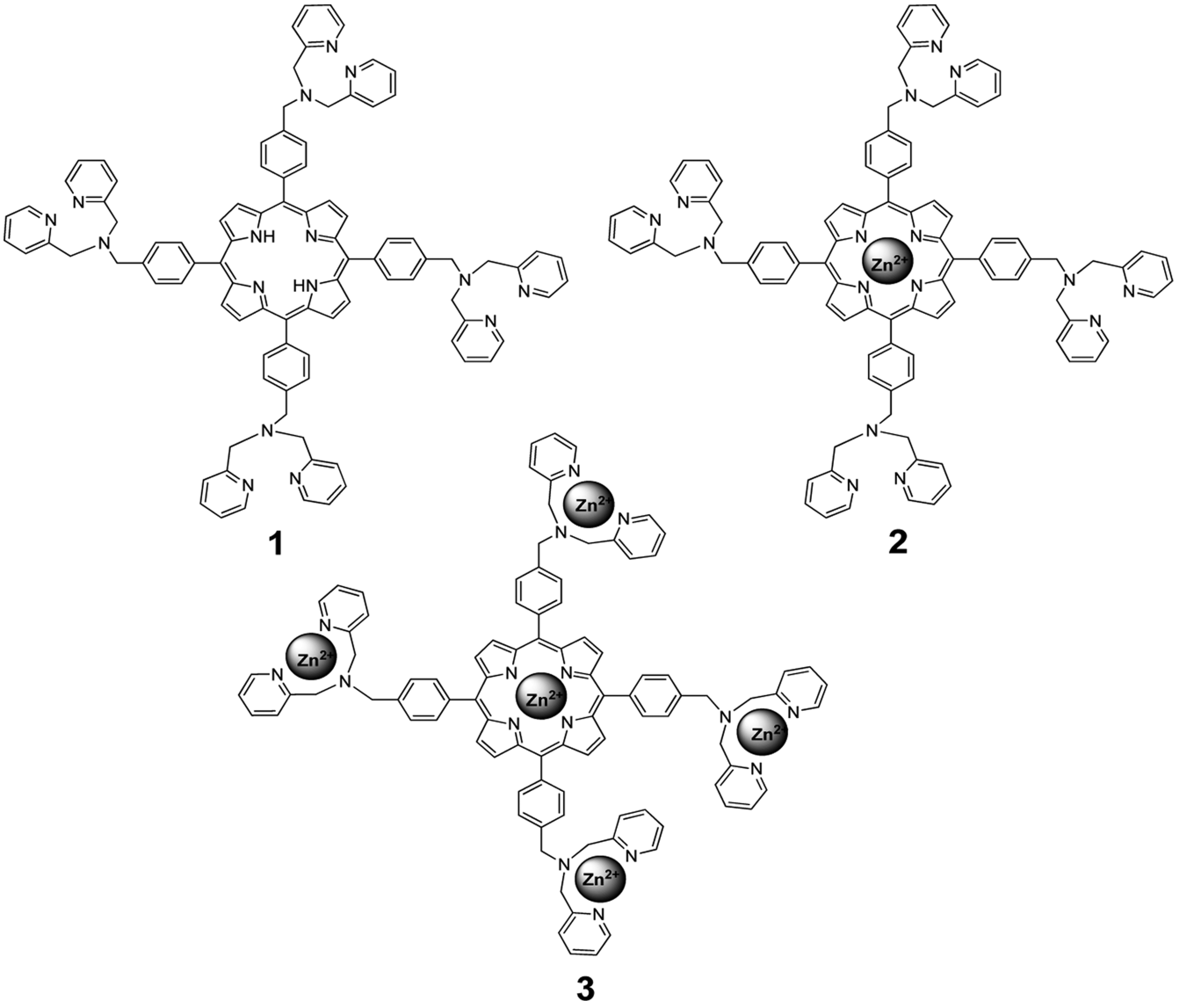

Recently, we have been involved in the development of efficient photosensitizers for photodynamic therapy as well as green photooxygenation reactions based on squaraines,[24−28] aza-BODIPYs,[29] and porphyrin systems.[30−34] Herein, we report a new series of the porphyrin conjugates **1**−**3** substituted with picolylamine groups as pendants (Chart 1) and have investigated the effect of heavy atom insertion on their intersystem crossing efficiency. Uniquely, the conjugate **3** with five zinc ions in the core as well as the pendant regions exhibited good solubility in the aqueous medium and quantitative yields of triplet excited states and singlet oxygen, thereby making it an ideal sensitizer for applications in photodynamic therapy and green photooxygenation processes.

2. EXPERIMENTAL SECTION

2.1. General Methods. The electronic absorption spectra were recorded on a Shimadzu UV-3101 or 2401PC UV−vis−NIR scanning spectrophotometer. The fluorescence spectra were recorded on a SPEX-Fluorolog F112X spectrofluorimeter. ^{1}H and ^{13}C NMR spectra were recorded on a 300 or 500 MHz Bruker advanced DPX spectrometer with chemical shifts reported relative to TMS.[35] All the solvents used were purified and distilled before use. Fluorescence quantum yields were determined through relative methods by using optically identical solutions, and hematoporphyrin (Φ_F = 0.01) was used as the standard in methanol.

2.2. Materials. *p*-Tolunitrile, *N*-bromosuccinimide (NBS), 2,2′-dipicolylamine, pyrrole, boron trifluoride diethyl etherate, triethylamine, zinc nitrate, rhuthenium trisbipyridyl, and *β*-carotene were purchased from Aldrich and S.D. Fine Chemicals, India. 1,3-Diphenylisobenzofuran (DPBF) was recrystallized from a mixture of EtOH/$CHCl_3$ (1:1). (2,2′-Dipicolylamino)methyl-5,10,15,20-tetrakis-phenylporphyrin, Zn(II)-(2,2′-dipicolylamino)methyl-5,10,15,20-tetrakis-phenylporphyrin, and Zn(II)$_5$-(2,2′-dipicolylamino)methyl-5,10,15,20-tetrakis-phenylporphyrin were synthesized according to the modified literature procedures.[36]

2.3. Synthesis of (2,2′-Dipicolylamino)methyl-5,10,15,20-tetrakis-phenylporphyrin (1). To a mixture of 5,10,15,20-tetrakis(*α*-bromo-*p*-tolyl)porphyrin (500 mg, 0.507 mmol), 2,2′-dipicolylamine (300 mg, 2.12 mmol), and K_2CO_3 (275 mg, 2.02 mmol) in anhydrous DMF (10 mL) was added

dx.doi.org/10.1021/jp407524w | J. Phys. Chem. B 2013, 117, 13515−13522

KI (82 mg, 0.507 mmol, dissolved in 4 mL of anhydrous DMF) dropwise over a period of 1 h at 25 °C. After stirring for 30 min at 25 °C, the reaction mixture was diluted with 1N HCl (15 mL) and washed twice with ethyl acetate. The aqueous layer was treated with 4N NaOH (50 mL) and extracted twice with a mixture (1:1) of ethyl acetate and THF. The combined organic layers were washed with water followed by being dried over Na_2SO_4. After the removal of the solvent under a vacuum, the residue was washed with toluene to remove the unreacted starting material. Further, the obtained residue was purified through recrystallization from a mixture (1:1) of dichloromethane and methanol to give purple colored porphyrin derivative **1** (76%). mp >300 °C. ^{1}H NMR (500 MHz, $CDCl_3$, TMS) (δ) −2.8 (s, 2H), 8.77 (s, 8H), 8.61 (d, 8H, J = 4.5 Hz), 8.14 (d, 8H, J = 7.5 Hz), 7.77 (t, 24H, J = 15 Hz), 7.22 (t, 8H, J = 11 Hz), 4.0 (d, 24H, J = 11.5 Hz). ^{13}C NMR (125 MHz, $CDCl_3$, TMS) δ 194.1, 159.4, 152.8, 150.7, 149.6, 138.9, 137.8, 135.3, 134.4, 128.7, 127.6, 124.1, 123.8, 122.7, 120.26, 60.24, 58.43, 50.97. HRMS (FAB): m/z Calcd for $C_{96}H_{82}N_{16}$, 1459.69; Found, 1461.52 $[M+2]^+$.

2.4. Synthesis of Zn(II)-(2,2′-dipicolylamino)methyl-5,10,15,20-tetrakis-phenylporphyrin (2). To a solution of 5,10,15,20-tetrakis(α-bromo-p-tolyl)porphyrin (200 mg, 0.2 mmol) in a mixture (3:1) of methanol and chloroform was added 1 equiv of zinc nitrate (0.2 mmol) dropwise over a period of 1 h, and the reaction mixture was stirred for 1 h at 25 °C. Evaporation of the solvent gave a residue, which was washed with chloroform and a mixture (1:1) of hexane and dichloromethane to remove the unreacted starting material. To a mixture of the above obtained product (200 mg, 0.19 mmol), 2,2′-dipicolylamine (95 mg, 0.48 mmol), and K_2CO_3 (105 mg, 0.76 mmol) in anhydrous DMF (10 mL), KI (31 mg, 0.19 mmol) dissolved in 4 mL of DMF was added dropwise over a period of 1 h at 25 °C. After stirring the reaction mixture for 30 min, it was diluted with 1N HCl (15 mL) and washed twice with ethyl acetate. The aqueous layer was treated with 4N NaOH (50 mL) and extracted twice with a mixture (1:1) of ethyl acetate and THF. The combined organic layers were washed with water followed by being dried over Na_2SO_4. After the removal of the solvent under a vacuum, the residue was washed with toluene to remove the unreacted starting material. The compound **2** (80%) thus obtained was further purified through recrystallization from a mixture (1:1) of dichloromethane and methanol. mp >300 ° C. ^{1}H NMR (500 MHz, CD_3OD, TMS) (δ) 8.65 (s, 8H), 8.41 (d, 8H, J = 4.5 Hz), 7.73 (t, 16H, J = 15 Hz), 7.55 (d, 8H, J = 7.5 Hz) 7.21 (t, 8H, J = 12 Hz), 3.90 (s, 16H), 3.81 (s, 8H). ^{13}C NMR (125 MHz, DMSO-d^6, TMS) δ 165.9, 161.7, 156.2, 152.5, 150.3, 149.8, 148.1, 137.8, 136.7, 128.4, 126.6, 124.5, 123.1, 122.9, 122.7, 99.4, 52.1, 44.1. MALDI-TOF MS: m/z Calcd for $C_{96}H_{80}N_{16}Zn$, 1523.12; Found, 1523.09 $[M^+]$.

2.5. Synthesis of (Zn(II))$_5$-(2,2′-dipicolylamino)methyl-5,10,15,20-tetrakis-phenylporphyrin (3). To a solution of **1** (200 mg, 0.13 mmol) in a mixture (3:1) of methanol and chloroform was added 5 equiv of zinc nitrate (0.65 mmol) dropwise, and the reaction mixture was allowed to stir for 1 h at 25 °C. Evaporation of the solvent gave a residue which was washed with chloroform and a mixture (1:1) of hexane and dichloromethane to remove the unreacted starting material. The zinc complex **3** (84%) thus obtained was further purified through recrystallization from a mixture (1:1) of dichloromethane and methanol. mp >300 °C. ^{1}H NMR (500 MHz, CD_3OD, TMS) (δ) 8.94 (s, 8H), 8.84 (d, 8H, J = 5 Hz), 8.37 (d, 8H, J = 7.5 Hz), 8.30 (t, 8H, J = 14.5 Hz), 7.96 (d, 8H, J = 8 Hz), 7.85 (t, 8H, J = 13 Hz), 7.68 (d, 8H, J = 7.5 Hz), 4.8 (d, 8H, J = 8 Hz), 4.24 (d, 8H, J = 16.5 Hz), 3.99 (s, 8H). ^{13}C NMR (125 MHz, DMSO-d^6, TMS) δ 172.9, 162.6, 151.9, 149.6, 149.4, 148.7, 139.1, 137.8, 128.7, 126.9, 124.1, 123.9, 123.4, 122.9, 122.3, 99.9, 50.8, 42.1. MALDI-TOF MS: m/z Calcd for $C_{96}H_{80}N_{16}Zn_5$, 1778.32; Found, 1778.48 $[M^+]$.

2.6. Nanosecond Laser Flash Photolysis. Nanosecond laser flash photolysis experiments were performed by using an Applied Photophysics model LKS-20 laser kinetic spectrometer using an OCR-12 Series Quanta Ray Nd:YAG laser. The laser beam source and the analyzer were fixed at right angles to each other, and the laser energy obtained was 60 mJ at 355 nm. The triplet quantum yields of the porphyrin derivatives were measured by using the energy transfer method, in which β-carotene was used as the energy acceptor from the porphyrin systems and $Ru(bpy)_3^{2+}$ as the standard. For the quantification of triplet energy, we used optically matching solutions of porphyrin derivatives and the reference $Ru(bpy)_3^{2+}$ at 355 nm.[37] To these solutions, an equal amount of known concentrations of β-carotene solution in THF was added. The transient absorbance (ΔA) of the β-carotene triplet absorption spectra, formed from the energy transfer from the reference and from the porphyrin derivatives, was monitored at 510 nm. Comparison of plateau absorbance following the completion of sensitized triplet formation, properly corrected for the decay of the donor triplets in competition with energy transfer to β-carotene, enabled us to estimate the triplet quantum yield (Φ_T) of the porphyrin derivatives by using the following equation:

$$\Phi_T^{por} = \Phi_T^{ref} \times (\Delta A_{por}/\Delta A_{ref}) \times (K_{obs}/K_{obs} - K_0)^{por} \times (K_{obs} - K_0/K_0)^{ref} \quad (1)$$

wherein the subscripts "ref" and "por" stand for reference $Ru(bpy)_3^{2+}$ and for the porphyrin derivatives, respectively, K_{obs} is the pseudo-first-order rate constant for the growth of the β-carotene triplet, and K_0 is the rate constant for the decay of the donor triplets in the absence of β-carotene observed in solutions of the reference or the porphyrin derivatives at the same optical density. Since β-carotene possesses a very negligible triplet yield, under similar experimental conditions, the direct excitation of β-carotene did not result in any significant triplet formation.

2.7. Quantification of Singlet Oxygen Yields. We carried out both direct and indirect methods to quantify singlet oxygen quantum yields. In the indirect method, we used a 200 W xenon lamp (model 3767) as a light source on an Oriel optical bench (model 11200) with a grating monochromator (model 77250). We were able to tune the intensity of light throughout the irradiations by measuring the output using an Oriel photodiode detection system (model 7072). The method we adopted here is the photooxidation of DPBF sensitized by the porphyrins, and the singlet oxygen generation quantum yields, Φ ($^1O_2$), of all derivatives were determined in methanol as solvent.[38] We measured the direct singlet oxygen emission intensity of the conjugates **1**−**3** and reference Hp by using a Fluorolog 3 spectrofluorimeter (FL3-221) connected with a NIR detector (Hamamatsu H10330A-45) with a 450 W xenon lamp as the light source. To obtain the direct singlet oxygen luminescence intensity by the steady-state method, we prepared optically matching solutions of **1**−**3** and Hp (OD − 0.1 ≤ x ≥ 0.15) in acetonitrile and used an excitation wavelength of 440

nm. We collected the emission in the 1100−1400 nm region with an integration time of 0.5 s/nm using a Hamamatsu H10330A-45 instrument.[39]

3. RESULTS AND DISCUSSION

3.1. Synthesis and Photophysical Properties. Synthesis of the picolylamine linked porphyrin derivative **1** was achieved in 76% yield by the reaction of picolylamine with tetrabromobenzylporphyrin which in turn was prepared by a modified Lindsey's method,[36] while the corresponding zinc complex **3** was synthesized in 84% yield by the reaction of **1** with 5 equiv of $Zn(NO_3)_2$ in methanol. Complex **2** having Zn^{2+} ions only in the porphyrin core was synthesized through the reaction of tetrabromobenzylporphyrin with 1 equiv of $Zn(NO_3)_2$, followed by its reaction with picolylamine.[40] All of these derivatives were purified and characterized on the basis of analytical and spectral evidence (Figures S1−S3, Supporting Information).

The absorption spectrum of compound **1** in methanol showed a characteristic porphyrin chromophore Soret band at 416 nm with a molar extinction coefficient of $(4.2 \pm 0.3) \times 10^5$ M^{-1} cm^{-1} and relatively weak Q bands in the region 510−650 nm. Similarly, complex **2** in methanol exhibited a bathochromically shifted Soret absorption band at 423 nm and Q bands at 557 and 595 nm, respectively. On the other hand, complex **3** having five zinc ions showed a sharp Soret band at 423 nm and two weak Q bands at 555 and 600 nm. The fluorescence spectra of **1** in methanol showed an emission maximum at 650 nm with a shoulder peak at 723 nm. In contrast, complexes **2** and **3** showed two blue-shifted emission maxima in the regions 610−615 and 655−658 nm, characteristic of the metalloporphyrin chromophore (Figure 1). We have determined the

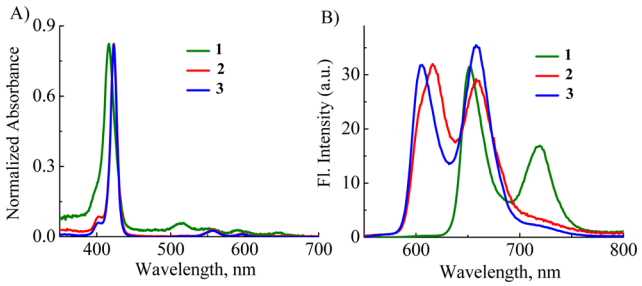

Figure 1. (A) Absorption and (B) fluorescence spectra of the porphyrin conjugates **1** (0.25 μM), **2** (0.5 μM), and **3** (0.8 μM) in methanol. λ_{ex} = 415 nm.

fluorescence quantum yields (Φ_F) of these derivatives, and the values are found to be 0.09, 0.029, and 0.028 for **1**, **2**, and **3**, respectively.[41] Among these compounds, **1** and **2** showed solubility in common organic solvents like chloroform, methanol, and dimethyl sulfoxide, whereas complex **3** showed good solubility in both organic solvents as well as in the aqueous media.

3.2. Characterization and Quantification of Triplet Excited State Properties. To understand the transient intermediates involved in the porphyrin conjugates **1**−**3**, we have carried out nanosecond laser flash photolysis studies under different conditions. Figure 2A shows the transient absorption spectrum of **1** in methanol, recorded after 355 laser pulse (50 mJ) excitation. The transient absorption showed an absorption maximum at 440 nm with a bleach at 416 nm, which corresponds to the ground state absorption of compound **1**

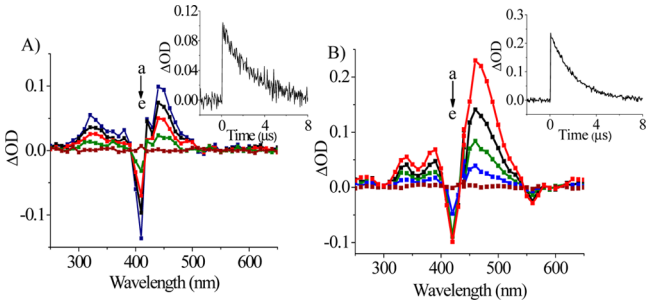

Figure 2. Transient absorption spectra in methanol of (A) **1** (0.46 μM) recorded at (a) 0.2, (b) 1.1, (c) 2.1, (d) 3.2, and (e) 10 μs and (B) **3** (0.51 μM) recorded at (a) 0.1, (b) 0.9, (c) 2, (d) 3.2, and (e) 11.5 μs following the 355 nm laser pulse excitation. The insets of parts A and B show the decay of the transients at 440 and 460 nm for **1** and **3**, respectively.

(Figure 2A). The transient intermediate from **1** decayed by a first-order process with a lifetime of 10 μs, leading to the recovery of the ground-state absorption of the compound. We have characterized the transient intermediate formed by saturating the methanolic solution of **1** with molecular oxygen. We observed the quenching of the transient absorption which clearly confirms that the transient species formed could be attributed to the triplet excited state of the compound.

Furthermore, we observed complete regeneration of the ground state absorption, thereby ruling out the formation of any other permanent products or the degradation of compound **1** under the laser excitation conditions. Similar studies were carried out with complexes **2** and **3** under identical conditions. We observed the transient absorption maximum, respectively, at 470 and 460 nm for **2** and **3**, with the triplet excited state lifetime values of 12 and 11 μs in methanol (Figure 2B and Figure S4, Supporting Information). The photophysical characteristics of these systems are summarized in Table 1.

To quantify the triplet excited state quantum yields (Φ_T) of the porphyrin conjugates **1**−**3**, we have adopted the triplet−triplet energy transfer method to β-carotene and have selected $[Ru(by)_3]^{2+}$ as the standard.[42] We have obtained triplet excited state quantum yields of ca. 0.64 ± 0.03 for the non-metalated derivative **1**, while ca. 0.92 ± 0.02 was observed for complex **2** which contains zinc metal ion in the porphyrin core. Interestingly, complex **3** having five Zn^{2+} metal ions both in the core as well as in the peripheral regions exhibited quantitative triplet excited state quantum yields of ca. 0.97 ± 0.02, thereby demonstrating the significant effect of the heavy atom substitution on the intersystem crossing efficacy of these derivatives (Table 1). We have carried out experiments with β-carotene alone which showed negligible transient absorption corresponding to its triplet excited state under similar experimental conditions (Figure S5, Supporting Information).

3.3. Tuning of Singlet Oxygen Generation Efficiency. Of particular interest for our present study is to evaluate the sensitized generation of singlet oxygen, since it is the key species responsible for photochemical and photobiological applications of various sensitizers. Therefore, we have quantified singlet oxygen efficiency of the porphyrin conjugates **1**−**3** using both direct and indirect methods. In the case of the indirect method, we have used 1,3-diphenylisobenzofuran (DPBF), a well-known singlet oxygen scavenger, and for the direct method, we quantified the luminescence of singlet oxygen at 1273 nm.[43] To carry out these experiments, we

Table 1. Photophysical Characteristics of the Picolylamine−Porphyrin Conjugates 1−3[a]

compound	λ_{max} (nm)	λ_{em} (nm)	Φ_F	τ (μs)	Φ_T	Φ_Δ[b]	Φ_Δ[c]
1	416	650,720	0.09 ± 0.01	10	0.64 ± 0.03	0.50 ± 0.03	0.59 ± 0.02
2	423	615,658	0.029 ± 0.02	12	0.92 ± 0.02	0.82 ± 0.04	0.85 ± 0.04
3	423	610,655	0.028 ± 0.01	11	0.97 ± 0.02	0.92 ± 0.03	0.95 ± 0.03

[a]Average of more than three experiments. [b]Denotes the singlet oxygen quantum yields obtained by the indirect (scavenging using 1,3-diphenylisobenzofuran, DPBF)[38] technique. [c]Denotes the singlet oxygen quantum yields obtained by the direct (quantifying the luminescence at 1273 nm)[19] technique.

irradiated an optically matched methanolic solution of the porphyrin **1** and DPBF using a 200 W mercury lamp with a 515 nm long pass over a time period of 0−60 s. The decrease in absorbance at 410 nm corresponding to DPBF in the presence of **1** was monitored. The singlet oxygen quantum yields were estimated by plotting the depletion in absorbance of DPBF against the irradiation time. This plot followed linearity, as shown in Figure 3B, and the experiment was done using

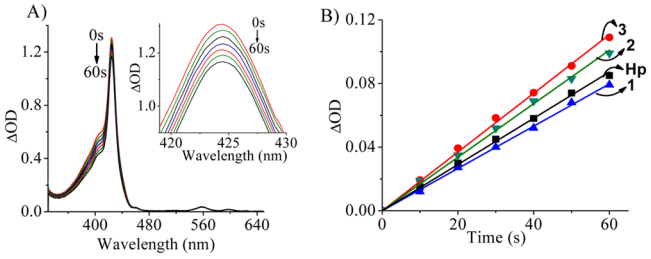

Figure 3. (A) Changes in absorption spectra of DPBF upon irradiation in the presence of **3** (3 μM) for 0−60 s (recorded at 10 s intervals) in methanol; λ_{ex} = 515 nm long pass filter. (B) Relative plot of the singlet oxygen generation efficacy of the porphyrin conjugates **1**, **2**, and **3** and the standard hematoporphyrin (Hp).

optically matching solutions of the compound as well as the reference. The singlet oxygen quantum yields were calculated by a relative method by comparing the photooxidation of DPBF sensitized by the dye to that of the reference, hematoporphyrin (Hp, Φ_Δ = 0.74),[44] using eq 2, wherein the superscripts "por" and "ref" represent for the porphyrin derivatives and reference, respectively.

$$\Phi(^1O_2)^{por} = \Phi(^1O_2)^{ref} \times [(m^{por} \times F^{ref})/(m^{ref} \times F^{por})] \quad (2)$$

The term "*m*" is the slope of a plot of difference in change in absorbance of DPBF at 410 nm with the irradiation time, and *F* is the absorption correction factor, $F = 1 - 10^{-OD}$, where OD is the optical density at the irradiation wavelength.

Similarly, we have carried out the scavenging of singlet oxygen by DPBF in the presence of complexes **2** and **3**. Figure 3B shows the relative plot of the changes in absorbance of DPBF vs the porphyrin conjugates **1**−**3** as well as the standard, hematoporphyrin (Hp). We observed that the free base porphyrin **1** showed a singlet oxygen quantum yield value of ca. 0.50 ± 0.03, whereas upon complexation with Zn^{2+} ions in the core resulted in a value of ca. 0.82 ± 0.04 for complex **2**. Interestingly, the incorporation of five Zn^{2+} ions, i.e., both at the core and at the peripheral units as in complex **3**, resulted in quantitative singlet oxygen quantum yields of ca. 0.92 ± 0.03. The porphyrin conjugates **1**−**3**, when irradiated alone and in the absence of DPBF, showed negligible changes at both Soret and Q absorption bands, thereby demonstrating their photostability under the experimental conditions (Figures 3 and 5A and Figures S6 and S7, Supporting Information).

For the direct measurement of singlet oxygen through the NIR luminescence method, we used a Fluorolog 3 spectrofluorimeter (FL3-221) connected with a NIR detector (Hamamatsu H10330A-45) and 450 W xenon lamp as the light source. To obtain the direct singlet oxygen luminescence intensity in the steady-state method, we prepared optically matched solutions of the porphyrin conjugates **1**−**3** and the reference Hp. Upon excitation at 440 nm, we observed the luminescence having a maximum at 1273 nm (Figure 4), which corresponds to singlet oxygen.[19] From the emission intensities of the conjugates **1**−**3** and Hp, the singlet oxygen quantum yields (Φ_Δ) were calculated by using eq 3

$$\Phi_{\Delta s} = (I_r/I_s) \times (I_{\Delta s}/I_{\Delta r}) \times (\tau_r/\tau_s) \times \Phi_{\Delta r} \quad (3)$$

wherein I_r and I_s denote for the incident light intensity and $I_{\Delta s}$ and $I_{\Delta r}$ represent the singlet oxygen luminescence intensity at 1273 nm for the porphyrin conjugates and the reference, respectively. τ_r and τ_s represent the lifetime of singlet oxygen in

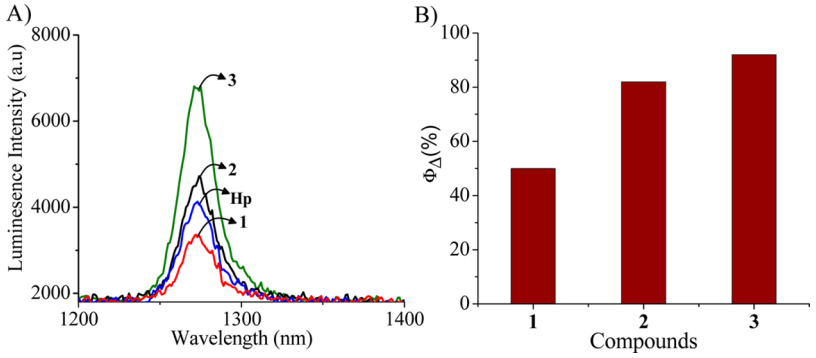

Figure 4. (A) Luminescence spectra of singlet oxygen observed at 1273 nm upon photoexcitation of the porphyrin conjugates **1** (0.32 μM), **2** (0.39 μM), and **3** (0.38 μM) and hematoporphyrin (Hp) (0.28 μM), λ_{ex} = 440 nm. (B) Histogram showing the percentage of singlet oxygen generated by **1**−**3** and quantified through luminescence at 1273 nm using a NIR photomultiplier tube (PMT).

dx.doi.org/10.1021/jp407524w | J. Phys. Chem. B 2013, 117, 13515−13522

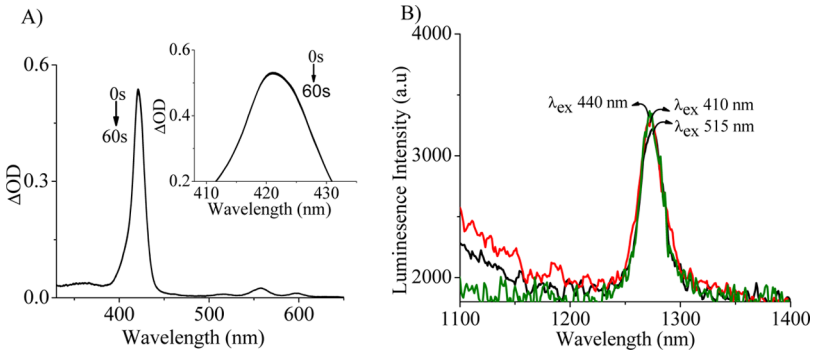

Figure 5. (A) Changes in absorbance of the porphyrin conjugate **3** (3 μM) upon irradiation (0−60 s) in the absence of 1,3-diphenylisobenzofuran (DPBF) and recording the spectrum at 10 s intervals. λ_{ex} = 515 nm using a long pass filter. (B) Luminescence spectra of singlet oxygen observed at 1273 nm upon photoexcitation of the porphyrin conjugate **1** (0.32 μM) using different excitation wavelengths, λ_{ex} = 410 (red), 440 (green), and 515 nm (black).

a particular solvent, and $\Phi_{\Delta r}$ is the singlet oxygen quantum yield of the reference, Hp. We observed singlet oxygen quantum yields of ca. 0.59 ± 0.02 for **1** and ca. 0.85 ± 0.04 for **2**. Interestingly, complex **3** having Zn^{2+} ions both in the core as well as in the periphery showed a quantitative singlet oxygen quantum yield of ca. 0.95 ± 0.03. To rule out the involvement of the third harmonic of the excitation wavelength at 1320 nm, we carried out measurements using different excitation wavelengths like 410 and 515 nm, and observed the same luminescence intensity and emission spectrum of singlet oxygen having a maximum at 1273 nm. This clearly indicates that the observed peak at 1273 nm is solely due to the direct emission of singlet oxygen, which is independent of the excitation wavelength (Figure 5B).

Interestingly, the efficiency of singlet-oxygen generation of the porphyrin conjugates **1**−**3** could be tuned by suitably incorporating Zn^{2+} metal ions at the core, as well as in the peripheral positions. We observed singlet-oxygen generation of ca. 0.50 ± 0.03 for the free base porphyrin derivative **1**, whereas the core metal ion insertion as in the case of **2** led to the enhancement in quantum yields of both the triplet excited state and singlet oxygen generation of ca. 0.92 ± 0.03 and 0.82 ± 0.04, respectively. The enhancement in the formation of triplet excited states and thereby the generation of singlet oxygen could be attributed to the increased intersystem crossing efficiency due to the presence of heavy metal ions.[45,46] Such an effect was further evidenced through the observation of the quantitative enhancement of the triplet excited state quantum yields of ca. 0.97 ± 0.02 and sensitized generation of singlet oxygen of ca. 0.92 ± 0.02 when five zinc metal ions were substituted as in the case of complex **3**. These results confirm that zinc metal ion plays a major role in the spin−orbit coupling interactions of the picolylamine linked porphyrin π-systems, and therefore, significantly enhanced rates of intersystem crossing efficiency were observed for complexes **2** and **3** when compared to the free base porphyrin conjugate **1**.

4. CONCLUSIONS

In summary, we have developed a new series of picolylamine linked porphyrin systems **1**−**3** and quantified their triplet excited states and singlet oxygen efficiency both directly and indirectly. By utilizing the heavy metal ion effect to improve the intersystem crossing efficiency, we introduced Zn^{2+} metal ions in the core (**2**) as well as in the periphery regions (**3**). Among the picolylamine linked porphyrin conjugates, complex **3** having five metal ions exhibited good water solubility and quantitative quantum yields of the triplet excited state (ca. 0.97 ± 0.02) and singlet oxygen generation efficiency (ca. 0.92 ± 0.03). These results clearly indicate that the insertion of Zn^{2+} ions can be effectively utilized in the picolyl−porphyrin systems to fine-tune their singlet oxygen yields, thereby demonstrating it as a simple approach for the design of efficient sensitizers for applications in photodynamic therapy and green photo-oxygenation reactions.

■ ASSOCIATED CONTENT

Supporting Information

Experimental details and Figures S1−S9 showing ^{1}H NMR, absorption, emission, and transient absorption spectra of the picolylamine linked porphyrin conjugates **1**−**3** under different conditions. This material is available free of charge via the Internet at http://pubs.acs.org.

■ AUTHOR INFORMATION

Corresponding Author

*E-mail: rama@niist.res.in or d.ramaiah@gmail.com.

Notes

The authors declare no competing financial interest.

■ ACKNOWLEDGMENTS

This work was supported by the Department of Science and Technology (DST), Government of India, and CSIR-National Institute for Interdisciplinary Science and Technology, Trivandrum 695019, India. This is Contribution No. PPG-344 from CSIR-NIIST, Trivandrum.

■ REFERENCES

(1) MacDonald, I. J.; Dougherty, T. J. Basic Principles of Photodynamic Therapy. *J. Porphyrins Phthalocyanines* **2001**, *5*, 105−129.

(2) Kadish, K. M.; Smith, K. M.; Guilard, R. Synthesis of meso substituted porphyrins. *The Porphyrin Handbook*; Academic Press: New York, 2002; Vol. *11*, pp 45−118.

(3) Bonnett, R. Photosensitizers of the Porphyrin and Phthalocyanine Series for Photodynamic Therapy. *Chem. Soc. Rev.* **1995**, *24*, 19−33.

(4) Johan, E. V.; Hongjian, T.; Hasrat, A.; Nicole, C.; Haroutioun, H. M. Trisulfonated Porphyrazines: New Photosensitizers for the Treatment of Retinal and Subretinal Edema. *J. Med. Chem.* **2009**, *52*, 4107−4110.

(5) Kelkar, S. S.; Reineke, T. M. Theranostics: Combining Imaging and Therapy. *Bioconjugate Chem.* **2011**, *22*, 1879−1903.
(6) Jovan, G.; Matibur, Z.; David, A.; Meyer, G. J.; Greer, A. Singlet Oxygen Chemistry in Water. 2. Photoexcited Sensitizer Quenching by O_2 at the Water-Porous Glass Interface. *J. Phys. Chem. B* **2008**, *112*, 15646−15650.
(7) Griesbeck, A. G.; Johannes, U.; Thomas, S.; Lhoussaine, B.; Reinhard, S.; Grundler, P. V.; Helm, L.; Alberto, R.; Merbatch, A. E. Singlet Oxygen Photo-Oxygenation in Water/Pluronic F-127 Hydrogels: Increased Reaction Efficiency Coupled with a Switch in Regioselectivity. *Chem.—Eur. J.* **2012**, *18*, 16161−16165.
(8) Fuckel, B.; Roberts, D. A.; Yuen, Y. C.; Raphae, G. C.; Roland, B. P.; Ekins-Daukes, N. J.; Maxwell, J. C.; Timothy, W. S. Singlet Oxygen Mediated Photochemical Upconversion of NIR Light. *J. Phys. Chem. Lett.* **2011**, *2*, 966−971.
(9) Foote, C. S. Photosensitized Oxygenations and the Role of Singlet Oxygen. *Acc. Chem. Res.* **1968**, *1*, 104−110.
(10) Ogilby, P. R. Singlet Oxygen: There is Indeed Something New under the Sun. *Chem. Soc. Rev.* **2010**, *39*, 3181−3209.
(11) Halina, A.; Beata, B. P.; Tondusson, M.; Eric, F. Ultrafast Dynamics of Metal Complexes of Tetrasulfonated Phthalocyanines at Biological Interfaces: Comparison between Photochemistry in Solutions, Films and Noncancerous and Cancerous Human Breast Tissues. *J. Phys. Chem. C* **2013**, *117*, 4999−5013.
(12) Ribeiro, A. O.; Tome, J. P. C.; Neves, M. S.; Cavaleiro, J. A. S.; Iamamoto, Y.; Torres, T. [1,2,3,4-Tetrakis(α/β-d-galactopyranos-6-yl)phthalocyaninato]zinc(II): A Water Soluble Phthalocyanines. *Tetrahedron Lett.* **2006**, *47*, 9177−9180.
(13) Bonnett, R.; Djelal, B. D.; Nguyen, A. Physical and Chemical Studies Related to the Development of m-THPC (FOSCAN®) for the Photodynamic Therapy (PDT) of Tumors. *J. Porphyrins Phthalocyanines* **2001**, *5*, 652−661.
(14) Lovell, J. F.; Liu, T. W.; Chen, J.; Zheng, G. Activatable Photosensitizers for Imaging and Therapy. *Chem. Rev.* **2010**, *110*, 2839−2857.
(15) Bonnett, R.; White, R. D.; Winfield, U. J.; Berenbaum, M. C. Hydroporphyrins of the Meso-tetra(hydroxyphenyl)porphyrin Series as Tumour Photosensitizers. *Biochem. J.* **1989**, *261*, 277−280.
(16) Griesbeck, A. G.; Alan de, K. A New Directing Mode for Singlet Oxygen Ene Reactions: The Vinylogous Gem Effect Enables a $^1O_2$ Domino Ene/[4 + 2] Process. *Org. Lett.* **2013**, *15*, 2073−2075.
(17) Ling, H.; Xuerong, Y.; Wanhua, W.; Jianzhang, Z. Styryl Bodipy-C_{60} Dyads as Efficient Heavy-Atom-Free Organic Triplet Photosensitizers. *Org. Lett.* **2012**, *14*, 2594−2597.
(18) Adarsh, N.; Shanmughasundaram, M.; Avirah, R. R.; Ramaiah, D. Aza-BODIPY Derivatives: Enhanced Quantum Yields of Triplet Excited States and the Generation of Singlet Oxygen and their Role as Facile Sustainable Photooxygenation Catalysts. *Chem.—Eur. J.* **2012**, *18*, 12655−12662.
(19) Sean, M.; Trevor, A. S.; Kenneth, P. G. Singlet Oxygen Quantum Yields of Potential Porphyrin Based Photosensitisers for Photodynamic Therapy. *Photochem. Photobiol. Sci.* **2007**, *6*, 995−1002.
(20) Silva, E. F. F.; Carlos, S.; Dabrowski, J. M.; Monteiro, C. J. P.; Formosinho, S. J.; Stochel, G.; Urbanska, K.; Simoes, S.; Mariette, M. P.; Arnaut, L. G. Mechanisms of Singlet Oxygen and Superoxide ion Generation by Porphyrins and Bacteriochlorins and Their Implications in Photodynamic Therapy. *Chem.—Eur. J.* **2010**, *16*, 9273−9286.
(21) Azenha, E. G.; Serra, A. C.; Pineiro, M.; Mariette, M. P.; Seixas de Melo, J.; Arnaut, L. G.; Formosinho, S.; Gonsalves, A. R. Heavy-atom Effects on Metalloporphyrins and Polyhalogenated Porphyrins. *Chem. Phys.* **2002**, *280*, 177−190.
(22) Daiana, K. D.; Christiane, P.; Eduardo, C.; Baptista, M. S.; Henrique, E. T.; Koti, A. Correlation of Photodynamic Activity and Singlet Oxygen Quantum Yields in Two Series of Hydrophobic Monocationic Porphyrins. *J. Porphyrins Phthalocyanines* **2012**, *16*, 55−63.
(23) Pavani, C.; Uchao, A. F.; Oliveira, C. S.; Iamamoto, Y.; Baptista, M. S. Effect of Zinc Insertion and Hydrophobicity on the Membrane Interactions and PDT Activity of Porphyrin Photosensitizers. *Photochem. Photobiol. Sci.* **2009**, *8*, 233−240.
(24) Avirah, R. R.; Dhanya, T. J.; Adarsh, N.; Ramaiah, D. Squaraine Dyes in PDT: From Basic Design to *In Vivo* Demonstration. *Org. Biomol. Chem.* **2012**, *10*, 911−920.
(25) Ramaiah, D.; Eckert, I.; Arun, K. T.; Weidenfeller, L.; Epe, B. Squaraine Dyes for Photodynamic Therapy: Mechanism of Cytotoxicity and DNA Damage Induced by Halogenated Squaraine Dyes Plus Light (>600 nm). *Photochem. Photobiol.* **2004**, *79*, 99−104.
(26) Ramaiah, D.; Eckert, I.; Arun, K. T.; Weidenfeller, L.; Epe, B. Squaraine Dyes for Photodynamic Therapy: Study of Their Cytotoxicity and Genotoxicity in Bacteria and Mammalian Cells. *Photochem. Photobiol.* **2002**, *76*, 672−677.
(27) Arun, K. T.; Ramaiah, D. Near-Infrared Fluorescent Probes: Synthesis and Spectroscopic Investigations of A Few Amphiphilic Squaraine Dyes. *J. Phys. Chem. A* **2005**, *109*, 5571−5578.
(28) Arun, K. T.; Epe, B.; Ramaiah, D. Aggregation Behavior of Halogenated Squaraine Dyes in Buffer, Electrolytes, Organized Media and DNA. *J. Phys. Chem. B* **2002**, *106*, 11622−11627.
(29) Adarsh, N.; Avirah, R. R.; Ramaiah, D. Tuning Photosensitized Singlet Oxygen Generation Efficiency of Novel Aza-BODIPY Dyes. *Org. Lett.* **2010**, *12*, 5720−5723.
(30) Suneesh, C. K.; Saneesh Babu, P. S.; Bollapalli, M.; Betsy, M.; Albish, K. P.; Asha, S. N.; Sridhar Rao, K.; Srinivasan, A.; Chandrashekar, T. K.; Mohan Rao, Ch.; et al. In Vitro Demonstration of Apoptosis Mediated Photodynamic Activity and NIR Nucleus Imaging through a Novel Porphyrin. *ACS Chem. Biol.* **2013**, *8*, 127−132.
(31) Nair, A. K.; Neelakandan, P. P.; Ramaiah, D. A; Supramolecular, Cu(II Metallocyclophane Probe for Guanosine 5′-monophoshate. *Chem. Commun.* **2009**, *42*, 6352−6354.
(32) Avirah, R. R.; Jyothish, K.; Ramaiah, D. Infrared Absorbing Croconaine Dyes: Synthesis and Metal Ion Binding properties. *J. Org. Chem.* **2008**, *73*, 274−279.
(33) Kuruvila, E.; Joseph, J.; Ramaiah, D. Novel Bifunctional Acridine-acridinium Conjugates: Synthesis and Study of Their Chromophore-selective Electron-transfer and DNA Binding Properties. *J. Phys. Chem. B* **2005**, *104*, 21997−22002.
(34) Takechi, K.; Kamat, P. V.; Avirah, R. R.; Jyothish, K.; Ramaiah, D. Harvesting Infrared Photons with Croconate Dyes. *Chem. Mater.* **2008**, *20*, 265−272.
(35) Jisha, V. S.; Arun, K. T.; Hariharan, M.; Ramaiah, D. Site-Selective Interactions: Squaraine Dye−Serum Albumin Complexes with Enhanced Fluorescence and Triplet Yields. *J. Phys. Chem. B* **2010**, *114*, 5912−5919.
(36) Littler, B. J.; Ciringh, Y.; Lindsey, J. S. Investigation of Conditions Giving Minimal Scrambling in the Synthesis of trans-Porphyrins from Dipyrromethanes and Aldehydes. *J. Org. Chem.* **1999**, *64*, 2864−2872.
(37) Joseph, J.; Eldho, N. V.; Ramaiah, D. Control of Electron-Transfer and DNA Binding Properties by the Tolyl Spacer Group in Viologen Linked Acridines. *J. Phys. Chem. B* **2003**, *107*, 4444−4450.
(38) Wolfgang, S.; Holger, K.; Dieter, W.; Steffen, H.; Beate, R.; Gunter, S. Singlet Oxygen Quantum Yields of Different Photosensitizers in Polar Solvents and Micellar Solutions. *J. Porphyrins. Phthalocyanines* **1998**, *2*, 145−158.
(39) Mark, N.; Michael, S. P.; Brian, C. W. Direct Near-infrared Luminescence Detection of Singlet Oxygen Generated by Photodynamic Therapy in Cells In Vitro and Tissues In Vivo. *Photochem. Photobiol.* **2002**, *75*, 382−391.
(40) Betsy, M.; Nair, A. K.; Ramaiah, D. Dye Encapsulation and Release by a Zinc−Porphyrin Pincer System through Morphological Transformations. *RSC Adv.* **2013**, *3*, 3815−3818.
(41) Harishankar, B.; Ramaiah, D. Dansyl—Naphthalimide Dyads As Molecular Probes: Effect of Spacer Group on Metal Ion Binding Properties. *J. Phys. Chem. B* **2011**, *115*, 13292−13299.
(42) Ramaiah, D.; Abraham, J.; Chandrasekhar, N.; Eldho, N. V.; Suresh, D.; George, M. V. Halogenated Squaraine Dyes as Potential Photochemotherapeutic Agents: Synthesis and Study of Photophysical

Properties and Quantum Efficiencies of Singlet Oxygen Generation. *Photochem. Photobiol.* **1997**, *65*, 783−790.
(43) Wozniak, M.; Tanfani, F.; Bertoli, E.; Zolese, G.; Antosiewicz, J. A New Fluorescence Method to Detect Singlet Oxygen Inside Phospholipid Model Membranes. *Biochim. Biophys. Acta* **1991**, *1*, 94−100.
(44) Redmond, R. W.; Gamlin, J. N. A Compilation of Singlet Oxygen Yields from Biologically Relevant Molecules. *Photochem. Photobiol.* **1999**, *70*, 391−475.
(45) Yishi, W.; Yonggang, Z.; Yuchao, M.; Renhui, Z.; Zhaohui, W.; Hongbing, F. Exceptional Intersystem Crossing in Di-(perylenebisimide)s: A Structural Platform toward Photosensitizers for Singlet Oxygen. *J. Phys. Chem. Lett.* **2010**, *1*, 2499−2502.
(46) Scott, W.; Davorin, P.; Honghua, H.; Lazaro, A. P.; Olga, V. P.; Artem, E. M.; Andriy, O. G.; Alexey, D. K.; Yurii, L. S.; Alexey, I. T.; et al. Near-Unity Quantum Yields for Intersystem Crossing and Singlet Oxygen Generation in Polymethine-like Molecules: Design and Experimental Realization. *J. Phys. Chem. Lett.* **2010**, *1*, 2354−2360.